

CircRNA LRIG3 knockdown inhibits hepatocellular carcinoma progression by regulating miR-223-3p and MAPK/ERK pathway

Type

Research paper

Keywords

hepatocellular carcinoma, miR-223-3p, circ_LRIG3, MAP2K6, MAPK/ERK pathway

Abstract

Introduction

Emerging evidence suggests that circular RNAs (circRNAs) play critical roles in tumorigenesis. However, the roles and molecular mechanisms of circRNA leucine-rich repeat immunoglobulin domain-containing protein 3 (circ_LRIG3) in hepatocellular carcinoma (HCC) has not been investigated.

Material and methods

The expression levels of circ_LRIG3, miR-223-3p, and mitogen-activated protein kinase kinase 6 (MAP2K6) were determined by qRT-PCR. Flow cytometry was applied to determine the cell cycle distribution and apoptosis. Cell proliferation, migration and invasion were assessed by MTT, colony formation, and transwell assays. Western blot assay was employed to measure the protein levels of the snail, E-cadherin, MAP2K6, mitogen-activated protein kinase (MAPK), phospho-MAPK (p-MAPK), extracellular signal-regulated kinases (ERKs), and phospho-ERKs (p-ERKs). The relationship between miR-223-3p and circ_LRIG3 or MAP2K6 was predicted by bioinformatics tools and verified by dual-luciferase reporter assay. A xenograft tumor model was established to confirm the functions of circ_LRIG3 in vivo.

Results

Circ_LRIG3 and MAP2K6 expression were enhanced while miR-223-3p abundance was reduced in HCC tissues and cells. Knockdown of circ_LRIG3 inhibited cell proliferation, metastasis, and increasing apoptosis. MiR-223-3p was a target of circ_LRIG3, and its downregulation reversed the inhibitory effect of circ_LRIG3 knockdown on the progression of HCC cells. Moreover, MAP2K6 could bind to miR-223-3p, and MAP2K6 upregulation also abolished the suppressive impact of circ_LRIG3 interference on progression of HCC cells. Additionally, the silence of circ_LRIG3 suppressed the activation of the MAPK/ERK pathway and tumor growth by upregulating miR-223-3p and downregulating MAP2K6.

Conclusions

Circ_LRIG3 knockdown inhibited HCC progression through regulating miR-223-3p/MAP2K6 axis and inactivating MAPK/ERK pathway.

1 **CircRNA LRIG3 knockdown inhibits hepatocellular carcinoma progression by**
2 **regulating miR-223-3p and MAPK/ERK pathway**

3

4 Hui Sun^{1,#}, Junwei Zhai^{2,#}, Li Zhang³, Yingnan Chen^{4,*}

5

6 ¹Department of Gastroenterology, Laiyang Central Hospital of Yantai City, Yantai 265200,
7 Shandong, China.

8 ²Department of Breast Surgery, Shandong Tengzhou Central People's Hospital, Tengzhou
9 277599, Shandong, China.

10 ³Department of Medical Rehabilitation, Heze Jiazheng Vocational College, Heze 2743000,
11 Shandong, China.

12 ⁴Department of Hepatic Surgery, Shandong Tengzhou Central People's Hospital, Tengzhou
13 277599, Shandong, China.

14

15 [#]These authors contributed equally to this paper.

16

17 ^{*}Corresponding Author: Yingnan Chen, Department of Hepatic Surgery, Shandong Tengzhou

18 Central People's Hospital, No.181 Xingtang Road, Tengzhou 277599, Shandong, China. Tel:

19 +86-0632-5633008. Email: sunhuish1111@163.com.

20

21

22

23 **Abstract**

24 **Introduction:** Emerging evidence suggests that circular RNAs (circRNAs) play critical roles
25 in tumorigenesis. However, the roles and molecular mechanisms of circRNA leucine-rich
26 repeat immunoglobulin domain-containing protein 3 (circ_LRIG3) in hepatocellular
27 carcinoma (HCC) has not been investigated.

28 **Methods:** The expression levels of circ_LRIG3, miR-223-3p, and mitogen-activated protein
29 kinase kinase 6 (MAP2K6) were determined by qRT-PCR. Flow cytometry was applied to
30 determine the cell cycle distribution and apoptosis. Cell proliferation, migration and invasion
31 were assessed by MTT, colony formation, and transwell assays. Western blot assay was
32 employed to measure the protein levels of the snail, E-cadherin, MAP2K6, mitogen-activated
33 protein kinase (MAPK), phospho-MAPK (p-MAPK), extracellular signal-regulated kinases
34 (ERKs), and phospho-ERKs (p- ERKs). The relationship between miR-223-3p and
35 circ_LRIG3 or MAP2K6 was predicted by bioinformatics tools and verified by
36 dual-luciferase reporter assay. A xenograft tumor model was established to confirm the
37 functions of circ_LRIG3 in vivo.

38 **Results:** Circ_LRIG3 and MAP2K6 expression were enhanced while miR-223-3p abundance
39 was reduced in HCC tissues and cells. Knockdown of circ_LRIG3 inhibited the progression
40 of HCC cells via reducing cell proliferation, metastasis, and increasing apoptosis.
41 MiR-223-3p was a target of circ_LRIG3, and its downregulation reversed the inhibitory effect
42 of circ_LRIG3 knockdown on the progression of HCC cells. Moreover, MAP2K6 could bind
43 to miR-223-3p, and MAP2K6 upregulation also abolished the suppressive impact of
44 circ_LRIG3 interference on progression of HCC cells. Additionally, the silence of

45 circ_LRIG3 suppressed the activation of the MAPK/ERK pathway and tumor growth by
46 upregulating miR-223-3p and downregulating MAP2K6.

47 **Conclusion:** Circ_LRIG3 knockdown inhibited HCC progression through regulating
48 miR-223-3p/MAP2K6 axis and inactivating MAPK/ERK pathway.

49 **Keywords:** hepatocellular carcinoma, circ_LRIG3, miR-223-3p, MAP2K6, MAPK/ERK
50 pathway

51

52 **Introduction**

53 Liver cancer is one of the most lethal and prevalent cancers worldwide, causing
54 approximately 745,500 deaths in 2012.¹ It has been reported that hepatocellular carcinoma
55 (HCC) is the main histological subtype of liver cancer and may cause a huge economic
56 burden.² Despite great advancement in therapeutic approaches, including surgery,
57 chemotherapy, and radiation therapy, the overall survival rate in advanced patients with HCC
58 is very poor.³ Therefore, it is critical to clarify the underlying mechanisms of HCC
59 progression and search new therapeutic strategies.

60 As a new type of endogenous non-coding RNA, circular RNA (circRNA) has become a
61 research hotspot in the RNA field and attracted widespread attention.⁴ Unlike linear RNAs,
62 circRNAs have covalently closed-loop structures with neither 5' cap nor 3' polyadenylated
63 tail and not easily affected by RNA exonuclease and more stable than linear RNAs.^{5,6} Up to
64 now, some studies have shown that circRNAs are extensively expressed in many types of
65 cells and participated in the progression and development of diverse cancers, including HCC.^{7,}

66 ⁸ For instance, circRNA Cdr1as served as an oncogene in HCC via regulating miR-7

67 expression.⁹ CircRNA cSMARCA5 could restrain HCC cell growth and metastasis.¹⁰ In
68 addition, circRNA leucine-rich repeat and immunoglobulin domain-containing protein 3
69 (circ_LRIG3; hsa_circ_0027345, chr12:59277301-59308117) has been reported to be
70 overexpressed in HCC tissues.¹¹ Nevertheless, the functional roles and molecular mechanisms
71 of circ_LRIG3 in HCC progression have not been clarified.

72 It has widely acknowledged that circRNAs can modulate gene expression via acting as
73 miRNA sponges in eukaryotes, which is one of the main mechanisms of physiological and
74 pathological processes.¹² MicroRNAs (miRNAs), a class of non-coding RNAs (~ 22
75 nucleotides), play regulatory roles in disease through interaction with mRNAs.¹³⁻¹⁶ MiR-223
76 has been identified to play an anti-cancer role in HCC and it might be a possible therapeutic
77 target for treating HCC.¹⁷ However, the connection between circ_LRIG3 and miR-223-3p has
78 not been reported. It has been suggested that mitogen-activated protein kinase kinase 6
79 (MAP2K6) can serve as a critical regulator in promoting tumorigenesis.¹⁸ Moreover, a
80 previous report verified that MAP2K6 had been shown to be among MAPKs upregulated in
81 various human HCC cohorts.¹⁹ However, the precise role of MAP2K6 in HCC cells is still
82 unclear. In our research, we first investigated the associations among miR-223-3p,
83 circ_LRIG3, and MAP2K6 in HCC cells.

84 Here, we measured miR-223-3p, circ_LRIG3, and MAP2K6 expression in HCC tissues and
85 cells, and determined their functions in HCC cells. Besides, we probed the
86 circ_LRIG3/miR-223-3p/MAP2K6 regulatory network in the progression of HCC. Our study
87 aimed to offer new insight into the diagnosis and treatment of HCC.

88

89 **Materials and methods**

90 **Specimens collection**

91 In our research, HCC tissues (n=46) and adjacent normal tissues (n=46) were acquired from
92 patients who underwent surgery at Laiyang Central Hospital of Yantai City. These tissues
93 were harvested and timely frozen in liquid nitrogen, and then preserved at -80°C until the
94 experiments were performed. These subjects did not receive any treatment and provided
95 informed **consent**. This procedure was granted by the Ethics Committee of Laiyang Central
96 Hospital of Yantai City.

97 **Cell culture and transfection**

98 Human HCC cell lines (Hep3B and Huh7) and human normal liver cell line (THLE-2) were
99 **obtained** from COBIOER (Nanjing, China). These cells were grown in Dulbecco's modified
100 eagle medium (DMEM; Hyclone, Logan, Utah, USA) supplemented with 10% fetal bovine
101 serum (FBS; Gibco, Carlsbad, CA, USA) in a **humidified** atmosphere with 5% carbon dioxide
102 at 37°C.

103 Small interfering RNA against circ_LRIG3 (si-circ_LRIG3) and its matched control (si-NC),
104 MAP2K6 overexpression plasmid (MAP2K6) and its matched control (pcDNA) were
105 synthesized by RIBOBIO (Guangzhou, China). Mimic or inhibitor of miR-223-3p
106 (miR-223-3p or anti-miR-223-3p) and mimic or inhibitor negative control (miR-NC or
107 anti-miR-NC) were provided by GenePharma (Jiangsu, China). Lentivirus-mediated shRNA
108 interference targeting circ_LRIG3 (sh-circ_LRIG3) and its matched control (sh-NC) were
109 **obtained** from Genechem (Shanghai, China). Lipofectamine 3000(Invitrogen, Carlsbad, CA,
110 USA) was used for cell transfection.

111 **Quantitative real-time polymerase chain reaction (qRT-PCR)**

112 Trizol reagent (Invitrogen) was utilized to obtain total RNA from tissue samples and cells.
113 For detecting genes expression, Prime Script RT reagent Kit (Takara, Dalian, China) and
114 TaqMan MicroRNA Reverse Transcription Kit (Thermo Fisher Scientific, Waltham, MA,
115 USA) was used to synthesizing the first strand of complementary DNA (cDNA). All reactions
116 were performed on the ABI 7300 system (Thermo Fisher Scientific) using the SYBR Green
117 PCR kit (Thermo Fisher Scientific). Primers for circ_LRIG3, LRIG3, miR-223-3p, MAP2K6,
118 U6, and glyceraldehyde-3-phosphate dehydrogenase (GAPDH) were exhibited as followed:

119 circ_LRIG3 forward (F, 5'- TCACTGGTTTGGATGCATTG-3'; R,
120 5'-AAGGTGGCTCATGGAACTTG-3'), LRIG3 (F,
121 5'-CACATCAATGGAACCTGGGTATTTTGAC-3'; R, 5'-
122 GTTTCGGTTCAATTCGAGATGTTGCAGTT-3'), miR-223-3p (F, 5'-
123 AGCTGGTGTGTGAATCAGGCCG-3'; R, 5'-TGGTGTCGTGGAGTCG-3'), MAP2K6,
124 (F, 5'-ATTTGGAGTCTGGGCATCAC-3'; R, 5'- ACTTGTCTGCTGGGAGTTGTG-3'),
125 GAPDH (F, 5'-CGCTCTCTGCTCCTCCTGTTC-3'; R,
126 5'-ATCCGTTGACTCCGACCTTCAC-3'), U6 (F,
127 5'-CTCGCTTCGGCAGCACATATACT-3'; R, 5'-ACGCTTCACGAATTTGCGTGTC-3').

128 The circ_LRIG3, LRIG3, MAP2K6, or miR-223-3p expression was assessed using the $2^{-\Delta\Delta Ct}$
129 method and standardized by GAPDH or U6, respectively.

130 **RNase R and Actinomycin D treatment**

131 To assess the stability of circ_LRIG3 and its linear isoform (LRIG3), dimethyl sulfoxide
132 solution (DMSO) or actinomycin D (2 mg/mL) was added to the cultured medium. RNase R

133 (3 U/μg, Epicentre Technologies, Madison, WI, USA) was utilized to incubate the total RNA
134 (2 μg) at 37°C for 30 min. After treatment with RNase R or Actinomycin D, these cells were
135 collected and then subjected to qRT-PCR for detecting the expression levels of circ_LRIG3
136 and LRIG3.

137 **Subcellular fractionation location**

138 PARIS Kit (Life Technologies Corp., Grand Island, NY, USA) was employed to isolate
139 cytosolic and nuclear fractions. In brief, Hep3B and Huh7 cells were carefully washed by
140 phosphate-buffered saline (PBS) and placed on the ice. Subsequently, these cells were
141 re-suspended in fractionation buffer and centrifuged at $500 \times g$ at 4°C for 5 min. Subsequently,
142 the cytoplasmic fraction would be separated from the nuclear pellet. After that, the remaining
143 nuclear pellet was again lysed by cell disruption buffer as the nuclear fraction. Lastly, the
144 abundance of U6, GAPDH and circ_LRIG3 was examined by qRT-PCR in the nuclear and
145 cytoplasmic fractions. GAPDH and U6 were served as controls for the cytoplasmic and
146 nuclear, respectively.

147 **Cell cycle assay**

148 Hep3B and Huh7 cells were collected following transfection for 48 h, and fixed by ice-cold
149 ethanol (70%) at -20°C for 24 h. Afterward, these cells were centrifuged and washed with
150 PBS, followed by staining with 25 μg/mL propidium iodide (PI) solution in PBS
151 supplemented with Triton X-100 (0.2%) and RNase A(50 μg/mL) for 20 min in the dark.
152 Lastly, flow cytometry (Guava Technologies, Hayward, CA, USA) was employed to examine
153 the cell cycle **distribution**.

154 **Cell proliferation assay**

155 Cell proliferation ability was evaluated using methylthiazolyldiphenyl-tetrazolium bromide
156 (MTT) assay. In short, Hep3B and Huh7 cells were placed in the 96-well plates overnight and
157 then transfected with si-NC, si-circ_LRIG3, si-circ_LRIG3 + anti-miR-NC, si-circ_LRIG3 +
158 anti-miR-223-3p, si-circ_LRIG3 + pcDNA, or si-circ_LRIG3 + MAP2K6. MTT solution (20
159 μ L, 5 mg/mL, Sangon Biotech, Shanghai, China) was added to per well following transfection
160 for 0 h, 24 h, 48 h, or 72 h. Following incubation for 4 h at 37°C, DMSO (150 μ L) was added
161 to per well after removing the cultured medium. The absorbance per well was examined with
162 the microplate reader (Bio-Teck, Winooski, VT, USA) at 490 nm.

163 **Colony formation assay**

164 In this assay, transfected Hep3B and Huh7 cells were introduced into six-well plates, followed
165 by incubation for two weeks at 37°C. After discarding the medium, cells were washed twice
166 with PBS (Invitrogen), and fixed using 70% ethanol for 30 min and stained using 0.1% crystal
167 violet for 5 min (Sigma-Aldrich, St. Louis, MO, USA). Finally, cell colonies were observed
168 and counted using a light microscope (Zeiss, Oberkochen, Germany).

169 **Cell apoptosis assay**

170 Annexin V-fluorescein isothiocyanate (FITC)/PI apoptosis detection kit (Sangon Biotech) was
171 applied to detect cell apoptosis according to the recommendations. In short, Hep3B and Huh7
172 cells were harvested and double-stained by Annexin V-FITC and PI for 20 min in the darkness.
173 Afterward, apoptotic cells were detected using a flow cytometer.

174 **Transwell assay**

175 Transwell chambers (pore size 8 μ m) (Corning Incorporation, Corning, NY, USA) coated
176 without and with Matrigel (BD Biosciences, San Jose, CA, USA) were utilized to assess

177 Hep3B and Huh7 cell migration and invasion abilities, respectively. In brief, cells were
178 suspended in serum-free medium (DMEM, 100 μ L) and then placed in the top surface of the
179 chamber, and DMEM mixed with FBS (10%) was placed in the bottom surface of the
180 chamber. Non-migrated or non-invaded cells from the top surface were gently wiped off using
181 cotton wool after incubation for 24 h. After that, the migrated or invaded cells were fixed
182 using paraformaldehyde (4%) and stained using crystal violet (0.1%). Lastly, a microscope
183 (Olympus, Tokyo, Japan) was utilized to photograph and count the migrated and invaded
184 cells.

185 **Western blot assay**

186 To extract the total protein, tissues or transfected cells were lysed by RIPA lysis buffer
187 (Sigma-Aldrich) containing 1mM phenylmethylsulphonyl fluoride (PMSF; Sigma-Aldrich).
188 After quantification by using the BCA protein assay kit (Thermo Fisher Scientific), protein
189 (about 40 μ g) was resolved by sodium dodecyl sulfate-polyacrylamide gel electrophoresis
190 (SDS-PAGE). **Afterward**, polyvinylidene fluoride (PVDF; Beyotime, Shanghai, China)
191 membranes were applied to transfer the protein. Next, membranes would be blocked using 5%
192 skim milk (Yili, Beijing, China) for 1 h, and then the membranes were probed with specific
193 primary antibody against snail (1:500, ab180714, Abcam, Cambridge, MA, USA), E-cadherin
194 (1:500, ab15148, Abcam), MAP2K6 (1:2000, ab154901, Abcam), mitogen-activated protein
195 kinase (MAPK) (1:1000, ab236738, Abcam), phospho-MAPK (p-MAPK) (1:500, ab47363,
196 Abcam), extracellular signal-regulated kinases (ERKs) (1:1000, ab17942, Abcam)
197 phospho-ERKs (p-ERKs) (1:1000, ab47339, Abcam), or GAPDH (1:2000, ab37168, Abcam)
198 overnight at 4°C. After that, these membranes were incubated by horseradish peroxidase

199 (HRP)-conjugated goat anti-rabbit immunoglobulin (Ig) G (1:4000, ab205718, Abcam).
200 Finally, all protein bands were observed with the enhanced chemiluminescence reagent
201 (Tanon, Shanghai, China). Relative protein expression was quantified by ImageJ software,
202 followed by normalizing to GAPDH expression.

203 **Dual-luciferase reporter assay**

204 Circinteractome (<https://circinteractome.nia.nih.gov/>) or TargetScan (www.targetscan.org)
205 software online was utilized to predict the potential binding sites of miR-223-3p and
206 circ_LRIG3 or MAP2K6. The circ_LRIG3 or MAP2K6 3'UTR fragments containing
207 wild-type (WT; containing the specific binding site with miR-223-3p) or mutant (MUT;
208 harboring the mutational binding sites with miR-223-3p) were amplified and cloned into
209 pmirGLO luciferase reporter vector (Cat. #E1330, Promega, Madison, WI, USA), namely WT
210 vectors (circ_LRIG3-wt, MAP2K6-wt) or MUT vectors (circ_LRIG3-mut, MAP2K6-mut).
211 Hep3B and Huh7 cells were co-transfected with those reporter vectors and miR-223-3p (or
212 miR-NC) for 48 h. Lastly, dual-luciferase assay system (Promega) was utilized for detecting
213 the luciferase activity, followed by normalizing to Renilla luciferase activity.

214 ***In vivo* tumor model**

215 The sh-circ_LRIG3 or sh-NC was transfected into Huh7 cells. Stably transfected cells (2×10^6)
216 were injected subcutaneously into BALB/c nude mice (n=6/group, male, six-week-old,
217 Shanghai Experimental Animal Center, Shanghai, China). From the 7th day, tumor length and
218 width were examined with a caliper every week and tumor volumes ($\text{length} \times \text{width}^2 \times 0.5$)
219 were calculated. After injection for 4 weeks, these mice would be sacrificed and tumor
220 specimens were weighed and collected for further analysis. The animal experiments obtained
221 approval from the Animal Care and Use Committee of Laiyang Central Hospital of Yantai
222 City.

223 **Statistical analysis**

224 In this study, all data from at least three **independent experiments** were displayed as mean \pm
225 standard deviation (SD). The significance of differences between groups was analyzed with
226 Student's *t*-test (for 2 groups) or a one-way analysis of variance (ANOVA; for more than 2
227 groups). Correlation between miR-223-3p and circ_LRIG3 or MAP2K6 was detected by
228 Spearman rank correlation. Statistical analyses were performed by Graphpad Prism version
229 6.0 software (GraphPad Software, San Diego, California, USA). $P < 0.05$ was considered to be
230 a statistically significant difference.

231

232 **Results**

233 **Circ_LRIG3 expression was increased in HCC tissues and cells**

234 To investigate the potential roles of circ_LRIG3 in HCC, its expression was examined in
235 HCC tissues and cells by qRT-PCR. Results displayed that the circ_LRIG3 level was
236 strikingly enhanced in HCC tissues in comparison with normal tissues (Figure 1A).
237 Similarly, its expression was also increased in HCC cells (Hep3B and Huh7) compared with
238 THLE-2 cells (Figure 1B). Next, we evaluated the stability of circ_LRIG3 in HCC cells.
239 According to the qRT-PCR analysis, circ_LRIG3 was resistant to RNase R relative to linear
240 LRIG3 in Hep3B and Huh7 cells (Figure 1C and 1D), implying that the circ_LRIG3 formed a
241 loop structure. Subsequently, Actinomycin D assay demonstrated that the half-life of
242 circ_LRIG3 transcript exceeded 24 h, indicating that circ_LRIG3 transcript was more stable
243 than the linear LRIG3 transcript in Hep3B and Huh7 cells (Figure 1E and 1F). Moreover, the
244 localization of circ_LRIG3 was analyzed in HCC cells. As presented in Figure 1G and 1H,

245 most of the circ_LRIG3 was located in the cytoplasm. These results suggested that
246 circ_LRIG3 might play critical roles in the progression of HCC.

247 **Knockdown of circ_LRIG3 inhibited cell proliferation, metastasis and induced apoptosis**
248 **in HCC cells**

249 To explore the effects of circ_LRIG3 on proliferation, metastasis and apoptosis of HCC cells,
250 si-NC or si-circ_LRIG3 was transfected into Hep3B and Huh7 cells. **The qRT-PCR analysis**
251 **results** showed that the expression of circ_LRIG3 was evidently reduced in Hep3B and Huh7
252 cells after transfection with si-circ_LRIG3, suggesting that transfection of si-circ_LRIG3 was
253 successful (Figure 2A and 2B). **Meanwhile, our data suggested that the knockdown of**
254 **circ_LRIG3 had no evident effect on linear LRIG3 level in Hep3B and Huh7 cells (Figure 2A**
255 **and 2B), implying that the expression of cir_LRIG3 is indeed silenced.** Cell cycle progression
256 was analyzed by flow cytometry, and cell proliferation was determined by MTT and colony
257 **formation assays.** Results displayed that the percentage of G0/G1 phase cells was increased
258 by downregulating circ_LRIG3, while the percentage of cells in S and G2/M phases **was**
259 reduced after the interference of circ_LRIG3 (Figure 2C and 2E), suggesting that the cell
260 cycle was arrested at the G0/G1 phase. MTT and **colony formation** analysis proved that cell
261 **proliferative ability** was obviously inhibited in Hep3B and Huh7 cells transfected with
262 si-circ_LRIG3 compared with those transfected with si-NC (Figure 2D, 2F, and 2G).
263 Moreover, we found that cell apoptosis was enhanced in Hep3B and Huh7 cells transfected
264 with si-circ_LRIG3 in contrast to the sh-NC group (Figure 2H). Transwell assay showed that
265 interference of circ_LRIG3 inhibited Hep3B and Huh7 cell migration and invasion (Figure 2I
266 **and 2J).** Western blot assay was applied to measure the metastasis-related proteins (snail and

267 E-cadherin). As depicted in Figure 2K and 2L, circ_LRIG3 silence decreased the protein level
268 of snail (a mesenchymal marker) while increased the protein expression of E-cadherin (an
269 epithelial marker) in Hep3B and Huh7 cells. These data collectively indicated that the
270 downregulation of circ_LRIG3 could inhibit the progression of HCC cells.

271 **MiR-223-3p was a direct target of circ_LRIG3**

272 A previous study indicated that circRNAs could act as molecular sponges of miRNAs in HCC
273 cells,²⁰ so the possible target miRNAs of circ_LRIG3 were predicted by the circinteractome
274 tool.²¹ As shown in Figure 3A, miR-223-3p was predicted as a target of circ_LRIG3. To
275 investigate whether miR-223-3p was a direct target of circ_LRIG3, we performed
276 dual-luciferase reporter assay in HCC cells. Results showed that transfection of miR-223-3p
277 mimic resulted in a significant reduction in luciferase activity of circ_LRIG3-wt compared to
278 miR-NC group, while the luciferase activity of circ_LRIG3-mut was unaffected by
279 transfection of miR-223-3p (Figure 3B and 3C). Next, we explored the impact of circ_LRIG3
280 on miR-223-3p expression. The results of qRT-PCR demonstrated that transfection of
281 si-circ_LRIG3 led to an obvious promotion of miR-223-3p expression, while co-transfection
282 of anti-miR-223-3p abated this effect (Figure 3D). Subsequently, the expression of
283 miR-223-3p was detected by qRT-PCR in HCC tissues and cells. As illustrated in Figure 3E
284 and 3F, the expression of miR-223-3p was downregulated in HCC cells and tissues compared
285 with their corresponding controls. Moreover, the correlation between miR-223-3p and
286 circ_LRIG3 expression was analyzed in HCC tissues. As displayed in Figure 3G, miR-223-3p
287 expression was negatively correlated with circ_LRIG3 level in HCC tissues ($r=-0.5054$,
288 $P=0.0003$). Thus, these results demonstrated that miR-223-3p was a target of circ_LRIG3 in

289 HCC cells.

290 **Knockdown miR-223-3p reversed the inhibitory effect of circ_LRIG3 downregulation**
291 **on the progression of HCC cells**

292 To explore whether the functions of circ_LRIG3 was mediated by miR-223-3p, Hep3B and
293 Huh7 cells were transfected with si-NC, si-circ_LRIG3, si-circ_LRIG3 + anti-miR-NC, or
294 si-circ_LRIG3 + anti-miR-223-3p. As shown in Figure 4A-4E, the effects of si-circ_LRIG3
295 on promotion of G0/G1 phase cells and reduction of S and G2/M phase's cells, and cell
296 **proliferative ability** were abolished by downregulating miR-223-3p. Moreover, the promotive
297 effect of circ_LRIG3 knockdown on apoptosis was abated by the downregulation of
298 miR-223-3p (Figure 4F). Transwell assay indicated that interference of miR-223-3p reversed
299 the inhibitory effects of circ_LRIG3 silence on migration and invasion (Figure 4G and 4H).
300 Likewise, downregulating miR-223-3p also could abrogate the effects of si-circ_LRIG3 on a
301 decrease of snail expression and increase of E-cadherin expression in Hep3B and Huh7 cells
302 (Figure 4I and 4J). These findings disclosed that circ_LRIG3 knockdown inhibited the
303 progression of HCC **cells** by up-regulating miR-223-3p.

304 **MAP2K6 is a target gene of miR-223-3p in HCC cells**

305 To further elucidate the mechanism of miR-223-3p in HCC cells, target prediction was
306 performed by TargetScan, and MAP2K6 was **identifying** as a candidate target for miR-223-3p
307 (Figure 5A). To further **determine** whether MAP2K6 was a direct target of miR-223-3p,
308 dual-luciferase reporter assay was carried out. We observed that the luciferase activity of
309 MAP2K6-wt was markedly suppressed in cells transfected with miR-223-3p, but luciferase

310 activity of MAP2K6-mut was not changed (Figure 5B and 5C). Transfection efficiency of
311 miR-223-3p and anti-miR-223-3p was measured by qRT-PCR. Results showed that
312 miR-223-3p expression was increased in cells transfected with miR-223-3p while its
313 expression was decreased in cells transfected with anti-miR-223-3p (Figure 5D), implying
314 that miR-223-3p and anti-miR-223-3p were successfully transfected in Hep3B and Huh7 cells.
315 Subsequently, the effect of miR-223-3p on the expression of MAP2K6 was explored. The
316 qRT-PCR and western blot analysis results showed that overexpression of miR-223-3p
317 reduced the MAP2K6 mRNA and protein expression, while knockdown of miR-223-3p
318 presented the opposite effect (Figure 5E and 5F). Next, the MAP2K6 mRNA and protein
319 expression were examined by qRT-PCR and western blot assays in HCC cells and tissues. The
320 results indicated that the mRNA and protein levels of MAP2K6 were overexpressed in HCC
321 cells and tissues compared with their matched controls (Figure 5G-5J). In addition, we found
322 that MAP2K6 mRNA expression was negatively correlated with miR-223-3p abundance
323 (Figure 5K) ($r=-0.5090$, $P=0.0003$). Furthermore, we investigated whether circ_LRIG3
324 functioned as a molecular sponge of miR-223-3p to regulate the expression of MAP2K6. We
325 observed that circ_LRIG3 deficiency decreased the mRNA and protein expression of
326 MAP2K6, while interference of miR-223-3p reversed this effect (Figure 5L and 5M).
327 Collectively, these data elaborated that circ_LRIG3 regulated MAP2K6 expression by
328 sponging miR-223-3p in HCC cells.

329 **Overexpression of MAP2K6 reversed the suppressive effect of si-circ_LRIG3 on the**
330 **progression of HCC cells**

331 To investigate whether MAP2K6 was involved in si-circ_LRIG3-mediated functions in HCC

332 cells, Hep3B and Huh7 cells were transfected with si-NC, si-circ_LRIG3, si-circ_LRIG3 +
333 pcDNA, or si-circ_LRIG3 + MAP2K6. As presented in Figure 6A and 6B, mRNA and protein
334 expression of MAP2K6 were reduced in cells transfected with si-circ_LRIG3 compared to
335 si-NC group, which was abated by the addition of MAP2K6. Flow cytometry, MTT, and
336 **colony formation** analysis showed that upregulation of MAP2K6 reversed the effects of
337 si-circ_LRIG3 on the promotion of G0/G1 phase cells and reduction of S and G2/M phases
338 cells as well as cell **proliferative ability** (Figure 6C-6G). Additionally, overexpression of
339 MAP2K6 abolished the pro-apoptosis, anti-migration and anti-invasion effects caused by
340 silencing circ_LRIG3 (Figure 6H-6J). Western blot assay proved that co-transfection of
341 MAP2K6 attenuated the suppression of snail expression and the promotion of E-cadherin
342 expression in Hep3B and Huh7 cells transfected with si-circ_LRIG3 (Figure 6K and 6L).
343 Therefore, we concluded that circ_LRIG3 knockdown suppressed the progression of HCC
344 cells by down-regulating MAP2K6.

345 **Silencing circ_LRIG3 inhibited the activation of MAPK/ERK pathway through**
346 **upregulating miR-223-3p and downregulating MAP2K6**

347 MAPK/ERK signaling pathway is known to be activated in many cancers.²²
348 MAPK/ERK-related proteins were analyzed by western blot assay. Results demonstrated that
349 knockdown of circ_LRIG3 reduced the protein levels of p-MAPK and p-ERKs, which was
350 reversed by the interference of miR-223-3p or overexpression of MAP2K6, but we observed
351 no change of total MAPK and ERKs protein in Hep3B and Huh7 cells (Figure 7A and 7B).
352 These findings indicated that circ_LRIG3 modulated the MAPK/ERK pathway by affecting
353 miR-223-3p and MAP2K6 expression.

354 **Knockdown of circ_LRIG3 limited tumor growth by regulating miR-223-3p and**
355 **MAP2K6 expression**

356 Sh-NC or sh-circ_LRIG3-transfected Huh7 cells were introduced into nude mice to assess the
357 role of circ_LRIG3 *in vivo*. As displayed in Figure 8A and 8B, the interference of circ_LRIG3
358 reduced tumor volume and weight in xenograft model. We then detected the expression of
359 circ_LRIG3, miR-223-3p, and MAP2K6 in tumor tissues. As shown in Figure 8C-8E,
360 silencing circ_LRIG3 decreased the expression of circ_LRIG3 and MAP2K6 while elevated
361 the abundance of miR-223-3p in excised tumor masses. Western blot assay also proved that
362 circ_LRIG3 interference led to a decrease of MAP2K6 protein expression in tumor tissues
363 (Figure 8F). **These results revealed** that circ_LRIG3 deficiency inhibited tumor growth via
364 upregulating miR-223-3p and downregulating MAP2K6 *in vivo*.

365
366 **Discussion**

367 HCC is one of the most common deadly cancers in the world. Growing evidence showed that
368 the abnormal expression of circRNAs was tightly related to tumorigenesis and the
369 development of tumors, including HCC.²³ Hence, more efforts should be made to deeply
370 explain the functional roles and underlying mechanisms of circ_LRIG3 in HCC. Here, we
371 found that circ_LRIG3 knockdown inhibited the progression of HCC by regulating the
372 miR-223-3p/MAP2K6 axis and inactivating MAPK/ERK signaling pathway.

373 Accumulating evidence has shown that circRNAs are abundant in eukaryotes and
374 **abnormally** expressed in human cancers.²⁴ **Because of** their covalently closed-structure,

375 circRNAs are more stable and more suitable as efficacious biomarkers than linear-RNAs,
376 such as lncRNAs and miRNAs.²⁵ For instance, circ_UVRAG,²⁶ circ_BACH2²⁷ and
377 circ_ANKS1B²⁸ have been identified as diagnostic or prognostic biomarkers for gastric
378 cancer, papillary thyroid carcinoma and breast cancer, respectively. A previous report has been
379 demonstrated that hsa_circ_0027345 (a circRNA derived from linear LRIG3) was
380 overexpressed in HCC tissues.¹¹ However, there is no report on the functions and underlying
381 mechanism of circ_LRIG3 in HCC. Consistent with the previous report, we also uncovered
382 that the circ_LRIG3 level was enhanced in HCC tissues and cell lines. Additionally, we
383 observed that knockdown of circ_LRIG3 inhibited the progression of HCC cells by reducing
384 cell proliferation and metastasis, and promoting apoptosis. These findings suggested that
385 circ_LRIG3 might act as a tumor promoter in HCC.

386 Emerging evidence showed that some circRNAs participated in tumorigenesis through
387 functioning as sponges for miRNAs.^{20, 29} Then, circinteractome was utilized to predict the
388 potential targets of circ_LRIG3. The data showed that circ_LRIG3 might interact with
389 miR-223-3p, which was validated using the dual-luciferase reporter assay in HCC cells.
390 MiR-223, a well-studied miRNA, presented different properties in different cancers, acting as
391 an oncogene in colorectal cancer,³⁰ gastric cancer³¹ and prostate cancer,³² or as an
392 anti-oncogene in esophageal carcinoma,³³ breast cancer³⁴ and osteosarcoma.³⁵ Previous
393 studies have suggested that miR-223 was lowly expressed HCC.^{36, 37} Moreover, miR-223 has
394 been suggested to repress HCC cell growth and accelerate apoptosis through the
395 Rab1-mediated mTOR activation.³⁸ In agreement with these findings, we proved that
396 miR-223-3p abundance was reduced in HCC tissues and cells, and its interference abated the

397 repressive impact of circ_LRIG3 downregulation on the progression of HCC cells. These data
398 suggested that circ_LRIG3 exerted its functions by sponging miR-223-3p in HCC cells.

399 It is well known that miRNAs mediate various cellular activities by regulating their
400 molecular targets.³⁹ Thus, the possible downstream targets of miR-223-3p were searched
401 through the TargetScan software. Our results revealed that MAP2K6 was a direct target of
402 miR-223-3p. MAP2K6 (important components of MAPK signal pathway) is involved in a
403 variety of physiological and pathological processes and drug resistance in human cancer cells.
404 It has been recognized as an oncogene in many cancers, such as esophageal
405 adenocarcinoma,⁴⁰ prostate cancer⁴¹, and colon cancers.¹⁸ However, the expression and effect
406 of MAP2K6 in HCC cells have not been clarified. Here, it was found that the MAP2K6 was
407 overexpressed in HCC tissues and cells, consistent with former work.¹⁹ And the expression
408 level of MAP2K6 was positively regulated by circ_LRIG3 and inversely modulated by
409 miR-223-3p. Functional experiments displayed that the upregulation of MAP2K6 abolished
410 the suppressive effect of circ_LRIG3 interference on the progression of HCC cells. Moreover,
411 *in vivo* experiments presented that circ_LRIG3 silence inhibited tumor growth through
412 upregulating miR-223-3p and downregulating MAP2K6 expression. Collectively, our results
413 disclosed that circ_LRIG3 knockdown repressed HCC progression by regulating the
414 miR-223-3p/MAP2K6 axis.

415 Previous studies show that HCC is associated with elevated expression and activity of
416 MAPK signaling intermediates (ie, MEK, ERK).⁴² Moreover, activation of the MAPK/ERK
417 signaling pathway predicted poor prognosis in HCC, and many anticancer agents exerted their
418 effects by blocking MAPK/ERK pathway.^{43, 44} These findings suggested that the MAPK/ERK

419 signaling pathway played key roles in HCC progression. In our research, results proved that
420 the knockdown of circ_LRIG3 repressed the activation of the MAPK/ERK signaling pathway
421 through up-regulating miR-223-3p and down-regulating MAP2K6.

422

423 **Conclusion**

424 In summary, we demonstrated that circ_LRIG3 and MAP2K6 were overexpressed and
425 miR-223-3p abundance was reduced in HCC tissues and cells. Circ_LRIG3 interference
426 limited cell growth and metastasis, and facilitated apoptosis in HCC cells through regulating
427 miR-223-3p/MAP2K6 axis and inactivating MAPK/ERK signaling pathway. These findings
428 might offer novel targets for treatment and prediction of HCC.

429 **Acknowledgement**

430 None.

431 **Disclosure of interest**

432 The authors declare that they have no financial conflict of interest.

433 **Funding**

434 None.

435 **References**

- 436 1. Torre LA, Bray F, Siegel RL, Ferlay J, Lortet - Tieulent J, Jemal A. Global cancer
437 statistics, 2012. CA Cancer J Clin. 2015;65:87-108.
- 438 2. Jinjuvadia R, Salami A, Lenhart A, Jinjuvadia K, Liangpunsakul S, Salgia R.
439 Hepatocellular carcinoma: a decade of hospitalizations and financial burden in the

- 440 United States. *Am J Med Sci.* 2017;354:362-369.
- 441 3. Altekruse SF, McGlynn KA, Reichman ME. Hepatocellular carcinoma incidence,
442 mortality, and survival trends in the United States from 1975 to 2005. *J Clin Oncol.*
443 2009;27:1485-1491.
- 444 4. Li X, Yang L, Chen L-L. The biogenesis, functions, and challenges of circular RNAs.
445 *Mol Cell.* 2018;71:428-442.
- 446 5. Memczak S, Jens M, Elefsinioti A, Torti F, Krueger J, Rybak A, et al. Circular RNAs are
447 a large class of animal RNAs with regulatory potency. *Nature.* 2013;495:333.
- 448 6. Chen L-L, Yang L. Regulation of circRNA biogenesis. *RNA Biol.* 2015;12:381-388.
- 449 7. Qin M, Liu G, Huo X, Tao X, Sun X, Ge Z, et al. Hsa_circ_0001649: a circular RNA and
450 potential novel biomarker for hepatocellular carcinoma. *Cancer Biomark.*
451 2016;16:161-169.
- 452 8. Meng S, Zhou H, Feng Z, Xu Z, Tang Y, Li P, et al. CircRNA: functions and properties
453 of a novel potential biomarker for cancer. *Mol Cancer.* 2017;16:94.
- 454 9. Yu L, Gong XJ, Sun L, Zhou QY, Lu BL, Zhu LY. The circular RNA Cdr1as act as an
455 oncogene in hepatocellular carcinoma through targeting miR-7 expression. *PLoS One.*
456 2016;11:e0158347.
- 457 10. Yu J, Xu QG, Wang ZG, Yang Y, Zhang L, Ma JZ, et al. Circular RNA cSMARCA5
458 inhibits growth and metastasis in hepatocellular carcinoma. *J Hepatol.*
459 2018;68:1214-1227.
- 460 11. Sun S, Wang W, Luo X, Li Y, Liu B, Li X, et al. Circular RNA circ-ADD3 inhibits
461 hepatocellular carcinoma metastasis through facilitating EZH2 degradation via

- 462 CDK1-mediated ubiquitination. *Am J Cancer Res.* 2019;9:1695-1707.
- 463 12. Hansen TB, Jensen TI, Clausen BH, Bramsen JB, Finsen B, Damgaard CK, et al. Natural
464 RNA circles function as efficient microRNA sponges. *Nature.* 2013;495:384-388.
- 465 13. Ardekani AM, Naeini MM. The role of microRNAs in human diseases. *Avicenna J Med*
466 *Biotechnol.* 2010;2:161.
- 467 14. Zhang H, Bao J, Zhao S, Huo Z, Li B. AURKAMicroRNA-490-3p suppresses
468 hepatocellular carcinoma cell proliferation and migration by targeting the aurora kinase
469 A gene (). *Arch Med Sci.* 2020;16:395-406.
- 470 15. Buranjiang G, Kuerban R, Abuduwanke A, Li X, Kuerban G. MicroRNA-331-3p inhibits
471 proliferation and metastasis of ovarian cancer by targeting RCC2. *Arch Med Sci.*
472 2019;15:1520-1529.
- 473 16. Fu W, Wu X, Yang Z, Mi H. The effect of miR-124-3p on cell proliferation and apoptosis
474 in bladder cancer by targeting EDNRB. *Arch Med Sci.* 2019;15:1154-1162.
- 475 17. Zhang C, Zhang J. Decreased expression of microRNA-223 promotes cell proliferation
476 in hepatocellular carcinoma cells via the insulin-like growth factor-1 signaling pathway.
477 *Exp Ther Med.* 2018;15:4325-4331.
- 478 18. Parray AA, Baba RA, Bhat HF, Wani L, Mokhdomi TA, Mushtaq U, et al. MKK6 is
479 upregulated in human esophageal, stomach, and colon cancers. *Cancer Invest.*
480 2014;32:416-422.
- 481 19. Nwosu ZC, Pioronska W, Battlro N, Zimmer AD, Dewidar B, Han M, et al. Severe
482 metabolic alterations in liver cancer lead to ERK pathway activation and drug resistance.
483 *EBioMedicine.* 2020;54:102699.

- 484 20. Kulcheski FR, Christoff AP, Margis R. Circular RNAs are miRNA sponges and can be
485 used as a new class of biomarker. *J Biotechnol.* 2016;238:42-51.
- 486 21. Dudekula DB, Panda AC, Grammatikakis I, De S, Abdelmohsen K, Gorospe M.
487 *CircInteractome: A web tool for exploring circular RNAs and their interacting proteins*
488 *and microRNAs. RNA Biol.* 2016;13:34-42.
- 489 22. Roy SK, Srivastava RK, Shankar S. Inhibition of PI3K/AKT and MAPK/ERK pathways
490 causes activation of FOXO transcription factor, leading to cell cycle arrest and apoptosis
491 in pancreatic cancer. *J Mol Signal.* 2010;5:10.
- 492 23. Bhan A, Soleimani M, Mandal SS. Long noncoding RNA and cancer: a new paradigm.
493 *Cancer Res.* 2017;77:3965-3981.
- 494 24. Shang Q, Yang Z, Jia R, Ge S. The novel roles of circRNAs in human cancer. *Mol*
495 *Cancer.* 2019;18:1-10.
- 496 25. Wang Y, Mo Y, Gong Z, Yang X, Yang M, Zhang S, et al. Circular RNAs in human
497 cancer. *Mol Cancer.* 2017;16:25.
- 498 26. Yang C, Wu S, Wu X, Zhou X, Jin S, Jiang H. Silencing circular RNA UVRAG inhibits
499 bladder cancer growth and metastasis by targeting the microRNA - 223/fibroblast
500 growth factor receptor 2 axis. *Cancer Sci.* 2019;110:99-106.
- 501 27. Cai X, Zhao Z, Dong J, Lv Q, Yun B, Liu J, et al. Circular RNA circBACH2 plays a role
502 in papillary thyroid carcinoma by sponging miR-139-5p and regulating LMO4
503 expression. *Cell Death Dis.* 2019;10:1-12.
- 504 28. Zeng K, He B, Yang BB, Xu T, Chen X, Xu M, et al. The pro-metastasis effect of
505 circANKS1B in breast cancer. *Mol Cancer.* 2018;17:1-19.

- 506 29. Subramanian S. Competing endogenous RNAs (ceRNAs): new entrants to the intricacies
507 of gene regulation. *Front Genet.* 2014;5:8.
- 508 30. Li ZW, Yang YM, Du LT, Dong Z, Wang LL, Zhang X, et al. Overexpression of miR-223
509 correlates with tumor metastasis and poor prognosis in patients with colorectal cancer.
510 *Med Oncol.* 2014;31:256.
- 511 31. Li J, Guo Y, Liang X, Sun M, Wang G, De W, et al. MicroRNA-223 functions as an
512 oncogene in human gastric cancer by targeting FBXW7/hCdc4. *J Cancer Res Clin Oncol.*
513 2012;138:763-774.
- 514 32. Wei Y, Yang J, Yi L, Wang Y, Dong Z, Liu Z, et al. MiR-223-3p targeting SEPT6
515 promotes the biological behavior of prostate cancer. *Sci Rep.* 2014;4:7546.
- 516 33. Li S, Li Z, Guo F, Qin X, Liu B, Lei Z, et al. miR-223 regulates migration and invasion
517 by targeting Artemin in human esophageal carcinoma. *J Biomed Sci.* 2011;18:24.
- 518 34. Yang Y, Jiang Z, Ma N, Wang B, Liu J, Zhang L, et al. MicroRNA-223 targeting STIM1
519 inhibits the biological behavior of breast cancer. *Cell Physiol Biochem.*
520 2018;45:856-866.
- 521 35. Ji Q, Xu X, Song Q, Xu Y, Tai Y, Goodman SB, et al. miR-223-3p inhibits human
522 osteosarcoma metastasis and progression by directly targeting CDH6. *Mol Ther.*
523 2018;26:1299-1312.
- 524 36. Karakatsanis A, Papaconstantinou I, Gazouli M, Lyberopoulou A, Polymeneas G, Voros
525 D. Expression of microRNAs, miR - 21, miR - 31, miR - 122, miR - 145, miR - 146a,
526 miR - 200c, miR - 221, miR - 222, and miR - 223 in patients with hepatocellular
527 carcinoma or intrahepatic cholangiocarcinoma and its prognostic significance. *Mol*

528 Carcinog. 2013;52:297-303.

529 37. Bhattacharya S, Steele R, Shrivastava S, Chakraborty S, Di Bisceglie AM, Ray RB.
530 Serum miR-30e and miR-223 as novel noninvasive biomarkers for hepatocellular
531 carcinoma. Am J Pathol. 2016;186:242-247.

532 38. Dong Z, Qi R, Guo X, Zhao X, Li Y, Zeng Z, et al. MiR-223 modulates hepatocellular
533 carcinoma cell proliferation through promoting apoptosis via the Rab1-mediated mTOR
534 activation. Biochem Biophys Res Commun. 2017;483:630-637.

535 39. Felekis K, Touvana E, Stefanou C, Deltas C. microRNAs: a newly described class of
536 encoded molecules that play a role in health and disease. Hippokratia. 2010;14:236-240.

537 40. Lin S, Liu K, Zhang Y, Jiang M, Lu R, Folts CJ, et al. Pharmacological targeting of p38
538 MAP-Kinase 6 (MAP2K6) inhibits the growth of esophageal adenocarcinoma. Cell
539 Signal. 2018;51:222-232.

540 41. Lotan T, Lyon M, Huo D, Taxy J, Brendler C, Foster B, et al. Up - regulation of MKK4,
541 MKK6 and MKK7 during prostate cancer progression: an important role for SAPK
542 signalling in prostatic neoplasia. J Pathol. 2007;212:386-394.

543 42. Wiesenauer CA, Yip-Schneider MT, Wang Y, Schmidt CM. Multiple anticancer effects of
544 blocking MEK-ERK signaling in hepatocellular carcinoma. J Am Coll Surg.
545 2004;198:410-421.

546 43. Schmitz KJ, Wohlschlaeger J, Lang H, Sotiropoulos GC, Malago M, Steveling K, et al.
547 Activation of the ERK and AKT signalling pathway predicts poor prognosis in
548 hepatocellular carcinoma and ERK activation in cancer tissue is associated with hepatitis
549 C virus infection. J Hepatol. 2008;48:83-90.

550 44. Liang RR, Zhang S, Qi JA, Wang ZD, Li J, Liu PJ, et al. Preferential inhibition of
551 hepatocellular carcinoma by the flavonoid Baicalein through blocking MEK-ERK
552 signaling. *Int J Oncol.* 2012;41:969-978.

553

554

555

556

557 **Figure Legends**

558 **Figure 1 The expression of circ_LRIG3 was enhanced in HCC tissues and cells.** (A) The
559 expression of circ_LRIG3 was determined in 46 pairs of HCC tissues and normal tissues
560 using qRT-PCR analysis. (B) The level of circ_LRIG3 was measured by qRT-PCR in HCC
561 cells (Hep3B and Huh7) and human normal liver cells (THLE-2). (C-F) The relative levels of
562 circ_LRIG3 and LRIG3 were determined after treatment with RNase R or actinomycin D by
563 qRT-PCR in Hep3B and Huh7 cells. (G and H) The qRT-PCR assay determined the
564 subcellular location of circ_LRIG3 in Hep3B and Huh7 cells. * $P < 0.05$.

565 **Figure 2 Knockdown of circ_LRIG3 inhibited the progression of HCC cells through**
566 **inhibiting cell proliferation and metastasis and promoting apoptosis.** Hep3B and Huh7
567 cells were transfected with si-NC or si-circ_LRIG3. (A and B) The expression of circ_LRIG3
568 and LRIG3 was analyzed by qRT-PCR. (C and E) Cell cycle distribution was analyzed using
569 the flow cytometry. (D and F) MTT assay was utilized to assess cell proliferation. (G) Colony
570 formation assay was used to detect cell proliferative ability. (H) Cell apoptosis was examined
571 using flow cytometry analysis. (I and J) Transwell assay was used to determine cell migration

572 and invasion abilities. (K and L) The protein levels of snail and E-cadherin were evaluated by
573 western blot assay. * $P < 0.05$.

574 **Figure 3 Circ_LRIG3 could interact with miR-223-3p in HCC cells.** (A) The putative
575 binding sites between circ_LRIG3 and miR-223-3p were predicted by circinteractome tool. (B
576 and C) Dual-luciferase luciferase reporter assay was utilized to detect the luciferase activity in
577 Hep3B and Huh7 cells co-transfected with circ_LRIG3-wt or circ_LRIG3-mut and miR-NC
578 or miR-223-3p mimic. (D) The expression of miR-223-3p was measured by qRT-PCR in
579 Hep3B and Huh7 cells transfected with si-NC, si-circ_LRIG3, si-circ_LRIG3 + anti-miR-NC,
580 or si-circ_LRIG3 + anti-miR-223-3p. (E and F) The abundance of miR-223-3p was analyzed
581 by qRT-PCR in HCC cells (Hep3B and Huh7), HCC tissues and their matched controls. (G)
582 The correlation between miR-223-3p abundance and circ_LRIG3 level was analyzed in HCC
583 tissues. * $P < 0.05$.

584 **Figure 4 Inhibition of miR-223-3p reversed the regulatory effect of circ_LRIG3**
585 **interference on the progression of HCC cells.** Hep3B and Huh7 cells were transfected with
586 si-NC, si-circ_LRIG3, si-circ_LRIG3 + anti-miR-NC, or si-circ_LRIG3 + anti-miR-223-3p.
587 (A and C) Cell cycle distribution was determined by flow cytometry. (B and D) MTT assay
588 was conducted to evaluate cell proliferation. (E) Colony formation assay was applied to assess
589 cell viability. (F) Cell apoptosis was measured by flow cytometry analysis. (G and H)
590 Transwell assay was employed to detect the number of migrated and invaded cells. (I and J)
591 Western blot analysis was applied to determine the protein levels of snail and E-cadherin.
592 * $P < 0.05$.

593 **Figure 5 MAP2K6 was targeted by miR-223-3p in HCC cells.** (A) The putative binding

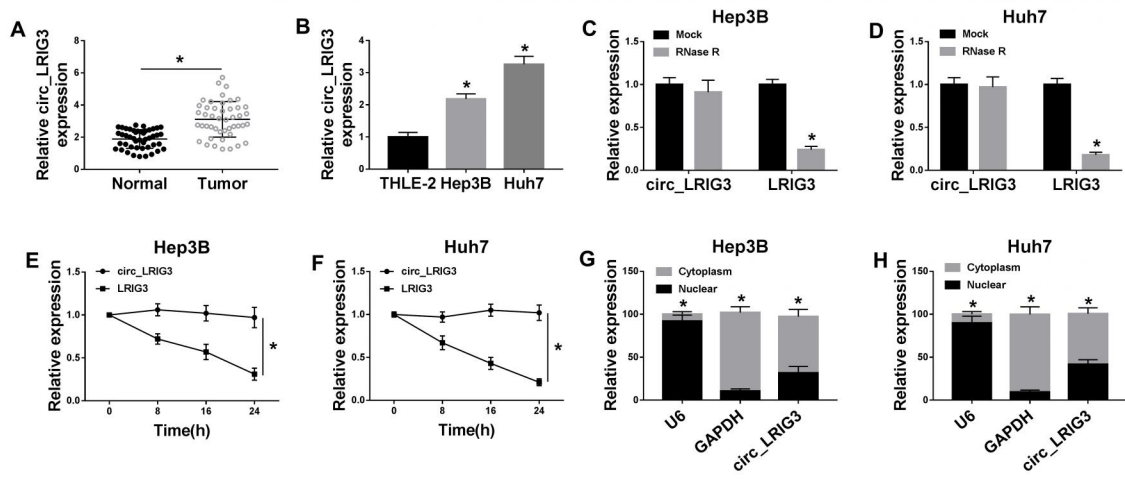
594 sequence of miR-223-3p in the 3'UTR of MAP2K6 was predicted by TargetScan. (B and C)
595 Relative luciferase activity was determined in Hep3B and Huh7 cells co-transfected with
596 MAP2K6-wt or MAP2K6-mut and miR-NC or or miR-223-3p mimic. (D) Relative
597 miR-223-3p expression was measured by qRT-PCR in Hep3B and Huh7 cells transfected with
598 miR-NC, miR-223-3p, anti-miR-NC, or anti-miR-223-3p. (E and F) MAP2K6 mRNA or
599 protein expression was analyzed by qRT-PCR or western blot assays in Hep3B and Huh7 cells
600 transfected with miR-NC, miR-223-3p, anti-miR-NC, or anti-miR-223-3p. (G and H) The
601 mRNA and protein levels of MAP2K6 were examined in HCC cells (Hep3B and Huh7) and
602 THLE-2 cells by qRT-PCR and western blot analyses, respectively. (I and J) QRT-PCR and
603 western blot assays were conducted to measure the mRNA and protein levels of MAP2K6 in
604 HCC tissues and normal tissues, respectively. (K) The association between miR-223-3p
605 abundance and MAP2K6 mRNA level was analyzed in HCC tissues. (L and M) The mRNA
606 and protein levels of MAP2K6 were detected in Hep3B and Huh7 cells transfected with si-NC,
607 si-circ_LRIG3, si-circ_LRIG3 + anti-miR-NC, or si-circ_LRIG3 + anti-miR-223-3p by
608 qRT-PCR and western blot analyses, respectively. * $P < 0.05$.

609 **Figure 6 Interference of circ_LRIG3 suppressed the progression of HCC cells by**
610 **downregulating MAP2K6.** Hep3B and Huh7 cells were transfected with si-NC,
611 si-circ_LRIG3, si-circ_LRIG3 + pcDNA, or si-circ_LRIG3 + MAP2K6. (A and B) The
612 mRNA and protein levels of MAP2K6 were measured by qRT-PCR and western blot analyses,
613 respectively. (C and E) Flow cytometry was applied to determine the cell cycle distribution.
614 (D and F) Cell proliferation was assessed by MTT analysis. (G) Cell proliferative ability was
615 detected by colony formation assay. (H) Cell apoptosis was determined using flow cytometry

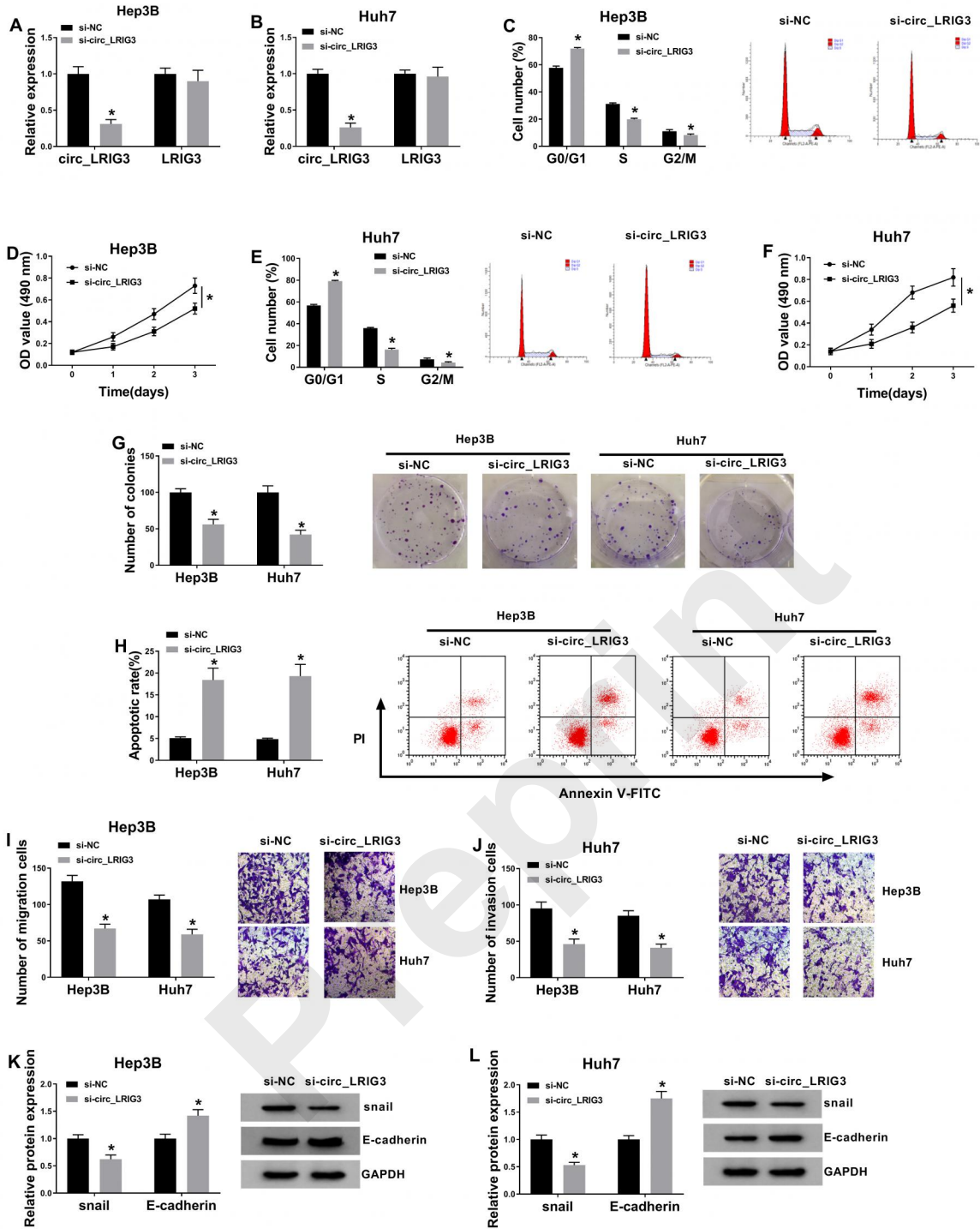
616 analysis. (I and J) Transwell assay was employed to count the number of migrated or invaded
617 cells. (K and L) The protein levels of snail and E-cadherin were tested by western blot
618 analysis. * $P < 0.05$.

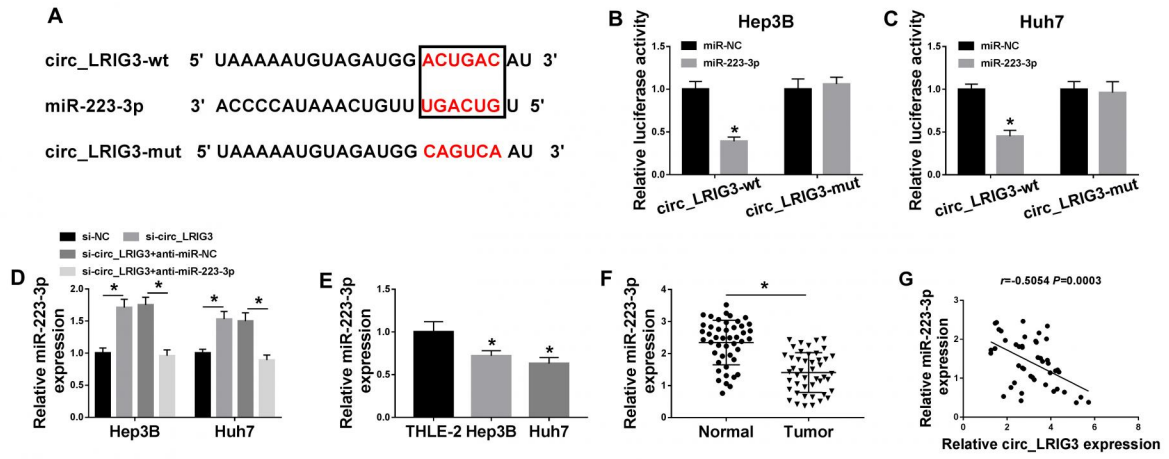
619 **Figure 7 Downregulation of circ_LRIG3 suppressed the activation of MAPK/ERK**
620 **pathway by regulating miR-223-3p and MAP2K6 expression.** (A and B) The protein levels
621 of MAPK, p-MAPK, ERKs, and p-ERKs were examined by western blot analysis in Hep3B
622 and Huh7 cells transfected with si-NC, si-circ_LRIG3, si-circ_LRIG3 + anti-miR-NC,
623 si-circ_LRIG3 + anti-miR-223-3p, si-circ_LRIG3 + pcDNA, or si-circ_LRIG3 + MAP2K6.
624 * $P < 0.05$.

625 **Figure 8 Silence of circ_LRIG3 repressed tumor growth by upregulating miR-223-3p**
626 **and downregulating MAP2K6.** Sh-NC or sh-circ_LRIG3-transfected Huh7 cells were
627 introduced into nude mice to establish mice model. (A and B) Tumor volume and weight were
628 examined. (C-E) The expression levels of circ_LRIG3, miR-223-3p and MAP2K6 were
629 determined by qRT-PCR in tumor tissues. (F) Western blot assay was applied to analyze the
630 protein expression of MAP2K6 in tumor tissues. * $P < 0.05$.

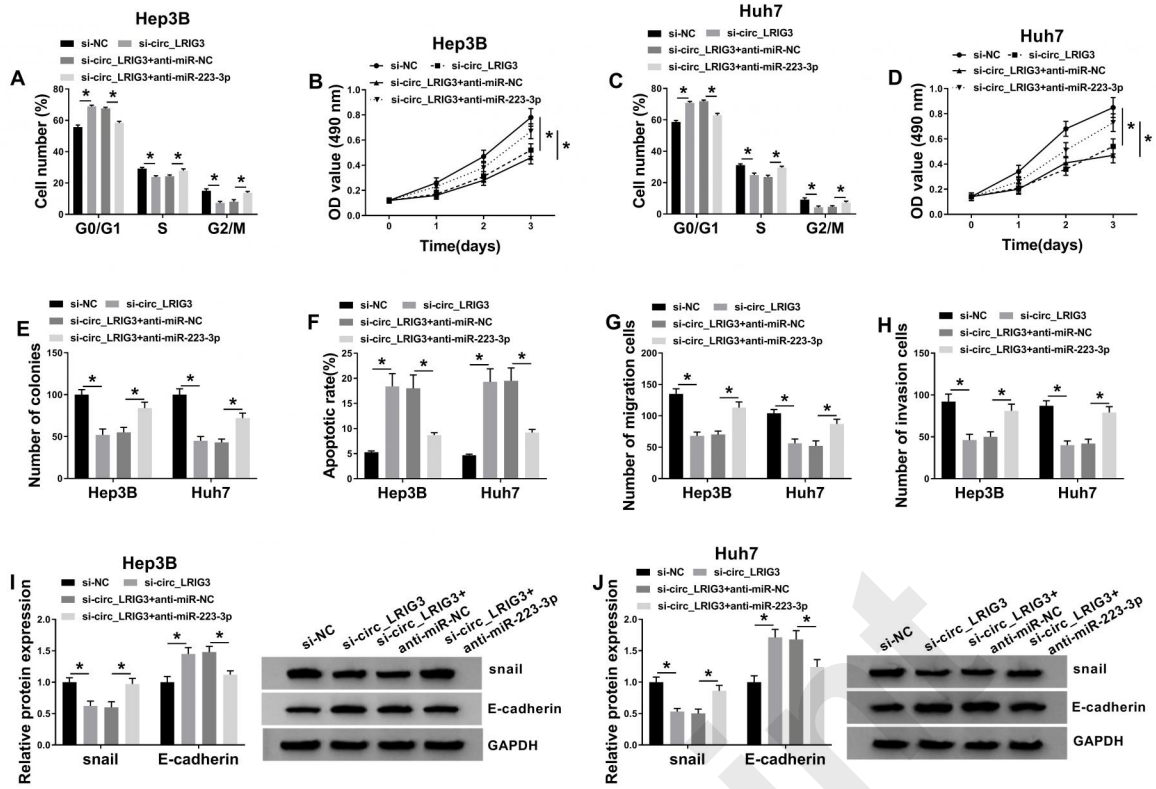


Preprint





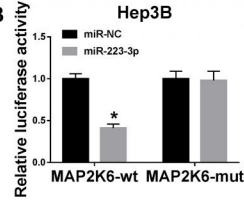
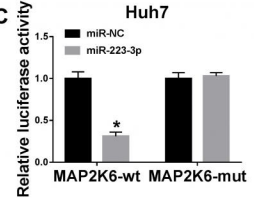
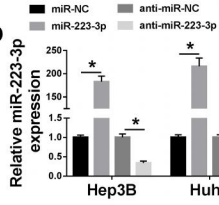
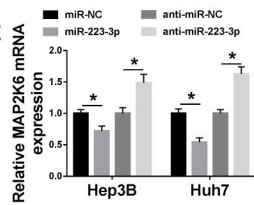
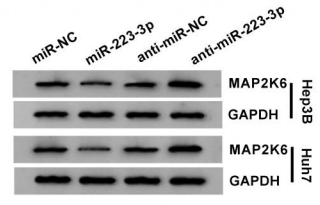
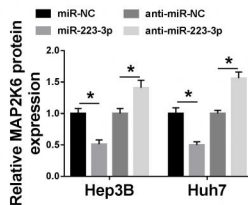
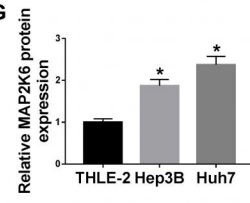
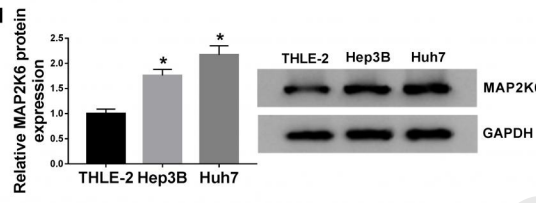
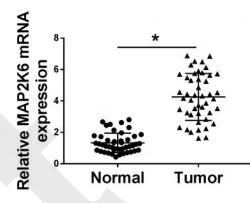
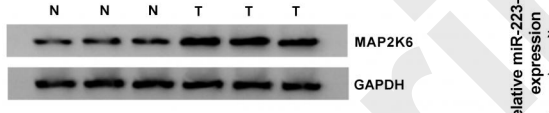
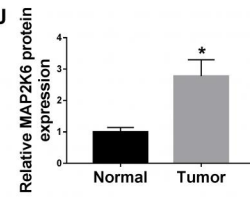
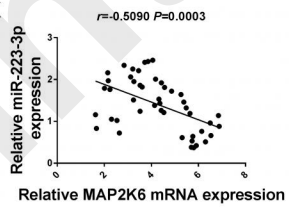
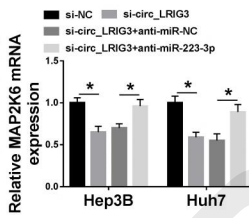
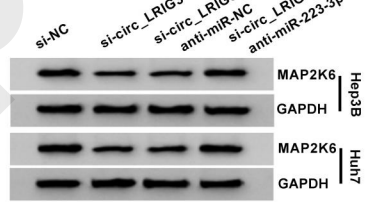
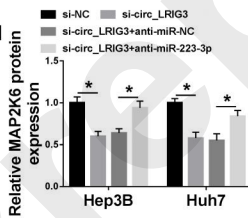
Preprint

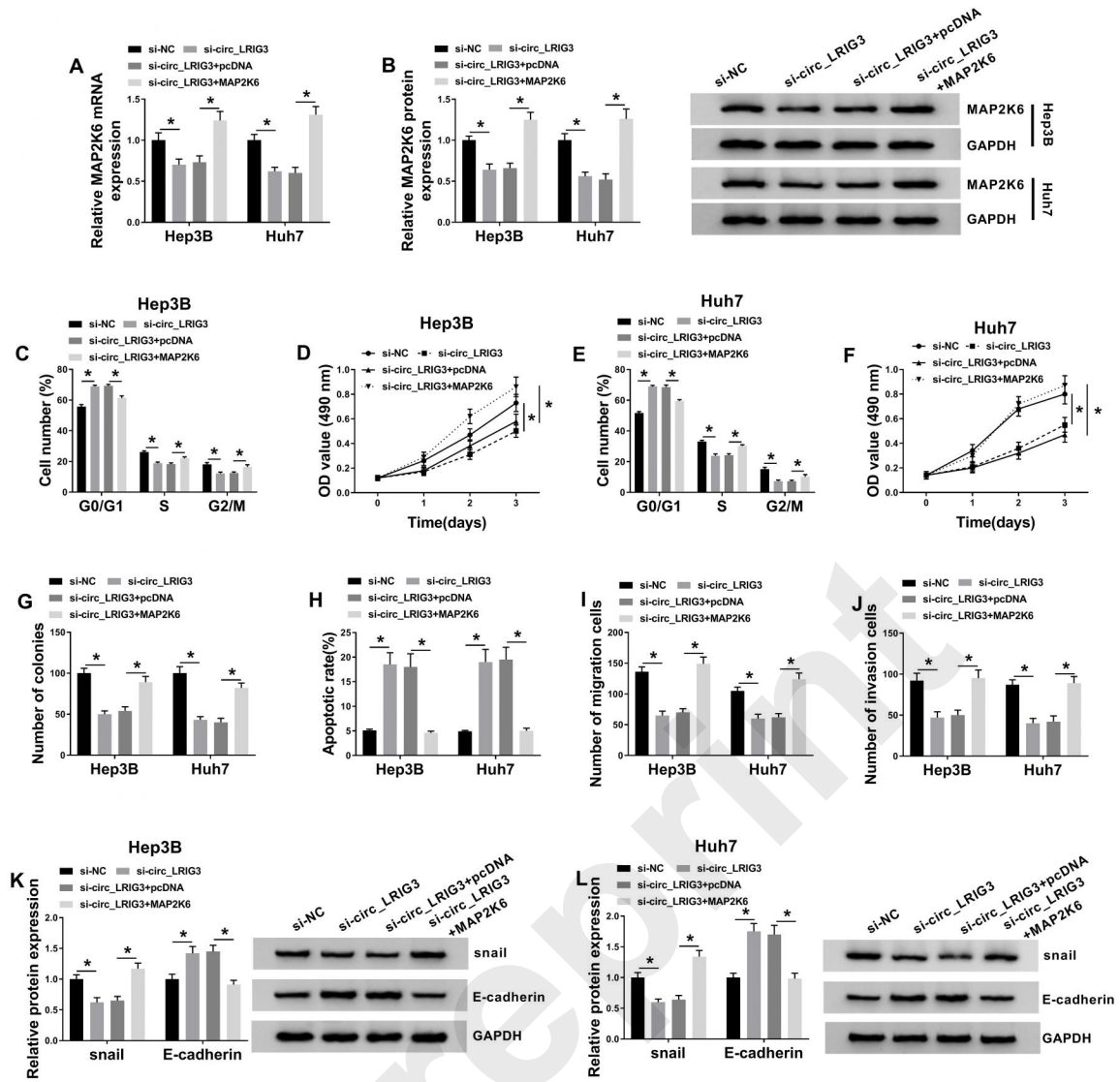


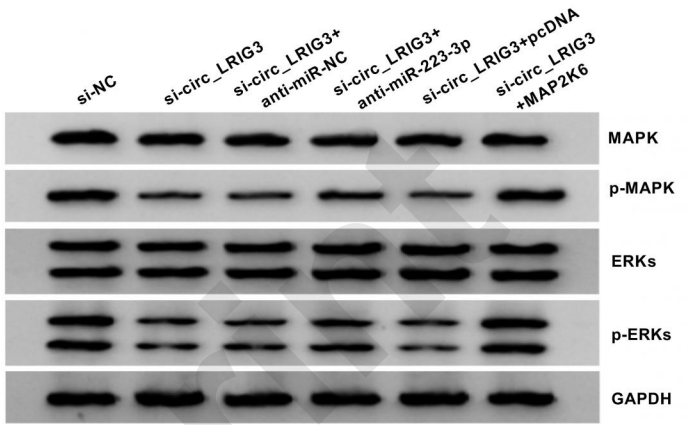
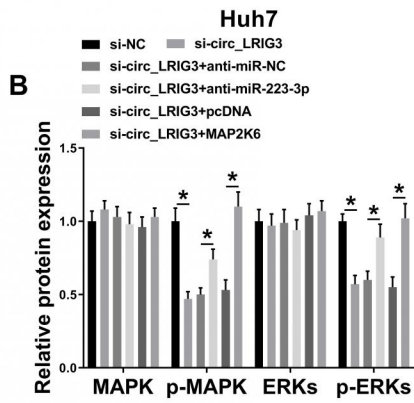
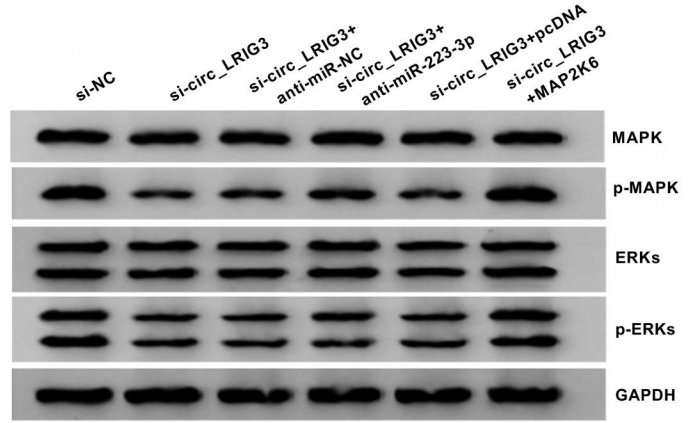
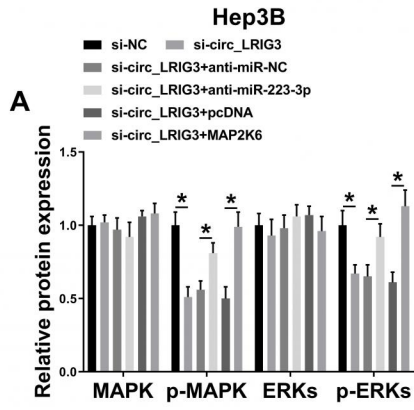
Preprint

A

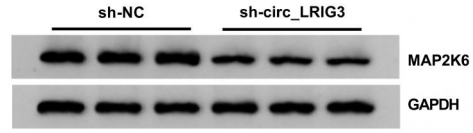
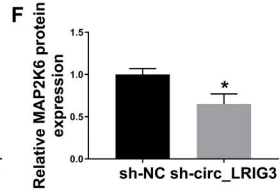
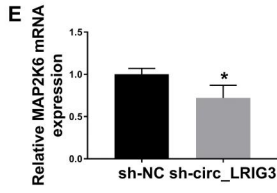
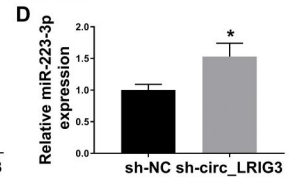
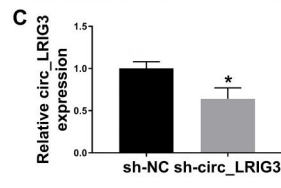
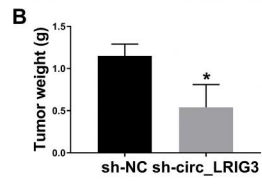
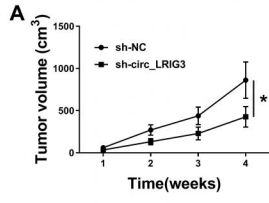
MAP2K6 3' UTR
 MAP2K6-wt 5' UUGUGUCAAUCUACA **AACUGAG** U 3'
 miR-223-3p 3' ACCCCAUAACUGU **UUGACUG** U 5'
 MAP2K6-mut 5' UUGUGUCAAUCUACA **CCAGUCA** U 3'

B**C****D****E****F****G****H****I****J****K****L****M**





Preprint



Preprint